Solvatochromic Analysis of Partition Coefficients in the *o*-Nitrophenyl Octyl Ether (*o*-NPOE)/Water System

by **Xiangli Liu**[a]), **Géraldine Bouchard**[a]), **Nathalie Müller**[a]), **Alexandra Galland**[a]), **Hubert Girault**[b]), **Bernard Testa**[a]), and **Pierre-Alain Carrupt***[a])

[a]) Institut de Chimie Thérapeutique, Section de Pharmacie, Université de Lausanne, BEP, CH-1015 Lausanne (fax: +41(0)21 692 45 25, e-mail: Pierre-Alain.Carrupt@ict.unil.ch)

[b]) Laboratoire d'Électrochimie Physique et Analytique, Ecole Polytechnique Fédérale de Lausanne, CH-1015 Lausanne

Dedicated to Professor *Duilio Arigoni* on the occasion of his 75th birthday

The objective of this study was to unravel the structural properties responsible for the partitioning of solutes in *o*-nitrophenyl octyl ether (*o*-NPOE)/H_2O, a new solvent system for the determination of the partition coefficients of ions. A set of 88 compounds (including drugs) was selected to allow a regular and broad distribution of property spaces. Partition coefficients in *o*-NPOE/H_2O ($\log P_{npoe}$) were measured by the shake-flask or the potentiometric method. Linear solvation free-energy relationship (LSER) analyses showed that *Van der Waals* volume, H-bond-acceptor basicity, and H-bond-donor acidity are the three molecular descriptors of solutes determining their $\log P_{npoe}$ values. The partitioning mechanism of the investigated compounds in *o*-NPOE/H_2O is controlled by the same structural properties as it is in 1,2-dichloroethane (DCE)/H_2O. $\Delta\log P_{oct-npoe}$ Values (difference between $\log P_{oct}$ and $\log P_{npoe}$) express mainly dipolarity/polarizability and H-bond-donor acidity. The solvent *o*-NPOE is shown to be a good candidate to replace DCE in measurements of lipophilicity.

1. Introduction. – The lipophilicity of solutes, as expressed by their partition coefficients, is very important from both physicochemical and biological viewpoints [1–3]. Partition properties represent the combined effects of a number of intermolecular forces between a solute and its environment.

The traditionally used measure of lipophilicity as a predictor of solute–membrane partitioning is the partition coefficient in the octanol/H_2O system ($\log P_{oct}$). In some studies, a relationship has been established between $\log P_{oct}$, and absorption or permeability in intestinal models [4][5], blood-brain-barrier models [6], and cell-culture models [7–10] to name a few. However, in many other situations, $\log P_{oct}$ cannot give a good estimate of a drug's absorption or permeation [11–15]. Thus, other solvent systems are needed to yield information that is complementary to $\log P_{oct}$ data. It is suggested that four classes of solvent systems are necessary to model the partitioning of solutes into membranes [16–18], namely *1*) an amphiprotic solvent such as octanol, *2*) a H-bond acceptor solvent such as dibutyl ether, *3*) a H-bond donor solvent such as $CHCl_3$, and *4*) an aprotic inert solvent such as alkane or 1,2-dichloroethane (DCE).

The classification of organic solvents given above implies that they interact differently with a given solute, resulting in different partition values. One highly informative interpretation of lipophilicity in different solvent/H_2O systems is the linear

solvation free-energy relationships (LSERs) based on the solvatochromic parameters [19–24]. LSERs can be expressed by the linear *Eqn. 1*.

$$\log P = v \cdot V_w + p \cdot \pi^* + a \cdot \alpha + b \cdot \beta + c \quad (1)$$

In this equation, the partition coefficient $\log P$ is factored into four structural parameters, namely a steric term (*Van der Waals* volume V_w), and polar terms known as solvatochromic parameters (dipolarity/polarizability π^*, H-bond-donor acidity α, and H-bond-acceptor basicity β). The steric term accounts for hydrophobic and dispersive forces, and the polar terms account for polar interactions between solutes and solvents. The regression coefficients v, p, a, and b reflect the relative contributions of each solute parameter to $\log P$.

To find more useful solvents for lipophilicity measurements, LSERs were used in this study to evaluate the intermolecular forces driving the partitioning of neutral organic solutes in *o*-nitrophenyl octyl ether (*o*-NPOE)/H_2O system. The solvent *o*-NPOE is used in voltammetry due to its remarkable physicochemical properties. Compared to 1,2-dichloroethane (DCE), another solvent traditionally used in voltammetry, it shows higher viscosity, lower volatility, lower solubility in H_2O, lower toxicity [25–26], and is stable over long periods [27]. A comparison of some physicochemical properties between *o*-NPOE and DCE can be seen in *Table 1*.

Table 1. *Comparison of Some Physicochemical Properties of* o-*Nitrophenyl Octyl Ether* (*o*-NPOE) *and 1,2-Dichloroethane* (DCE) *at 298 K* [25]

Properties	*o*-NPOE	DCE
Molar mass [$g \cdot mol^{-1}$]	251.33	98.96
Density [$g \cdot cm^{-3}$]	1.041[a])	1.246
Molar volume [$cm^3 \cdot mol^{-1}$]	241.4	79.4
Viscosity [10^{-3} Pa · s]	13.800	0.779
Solubility of the solvent in H_2O [$mol \cdot l^{-1}$]	2.01×10^{-6}	8.50×10^{-2}
Solubility of H_2O in the solvent [$mol \cdot l^{-1}$]	4.06×10^{-2}	0.11
Effective solvent radius [nm]	0.368	0.254
Relative permittivity	24.20	10.36

[a]) At 293 K.

In a previous study, a set of 80 compounds selected by cluster analysis [28] were used to unravel the structural determinants governing the partitioning of solutes in the DCE/H_2O system [24]. However, the distribution of structural parameters (V_w, π^*, β, α) in this set was too narrow with respect to the structural parameters describing drugs. In the present study, the set was extended by adding 74 molecules, including drugs (*Fig. 1*). The compounds in the extended set were rigid ones covering a broader range of V_w, π^*, β, and α values than the compounds in the initial set. This new set of compounds was used to develop a solvatochromic equation that factores partition coefficients. Moreover, the comparison between solvatochromic equations in the *o*-NPOE/H_2O, DCE/H_2O, and octanol/H_2O systems is also discussed.

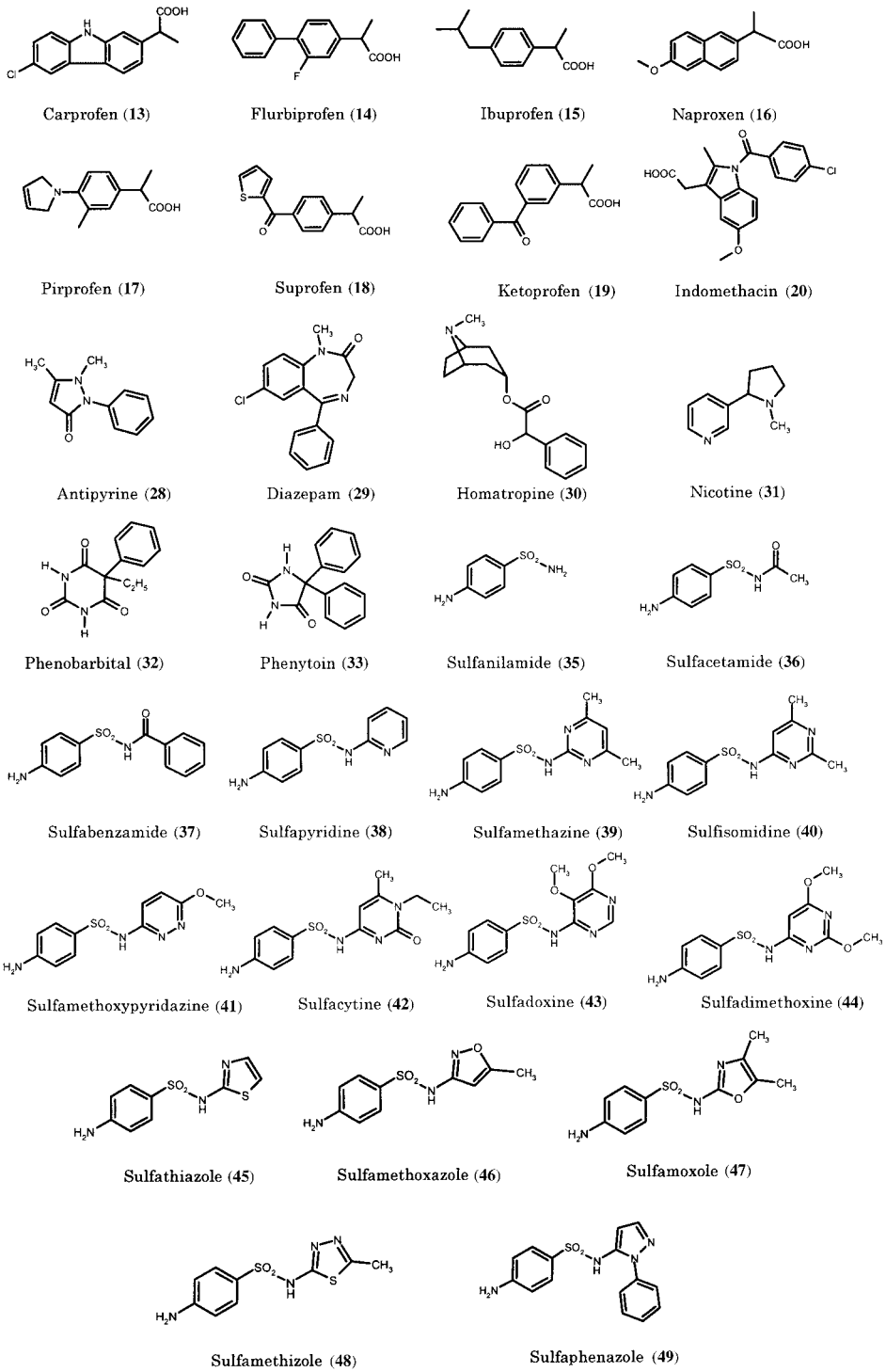

Fig. 1. *Structures of the complex compounds under investigation*

2. Results and Discussion. – 2.1. *Validation of the Solvatochromic Parameters Calculated by the Systahl 2.0 and Pistal 1.0 Fragmental Systems.* The solvatochromic parameters (π^*, β, α) were calculated by *ad hoc* fragmental systems (Systahl 2.0 and Pistal 1.0) due to the unavailability of experimental values for some compounds (*Table 2*). To verify the calculated parameters, the LSERs equations of $\log P_{npoe}$, $\log P_{dce}$, and $\log P_{oct}$ obtained with these calculated parameters (*T* log *P* in *Tables 3* and *4*) were compared with those obtained by the experimental parameters (log *P* in *Tables 3* and *4*) for the 41 compounds (compounds **22**, **24**, and **50**–**88**) representing the original set [24]. The regression coefficients (together with the 95% confidence limits) and the statistics are shown in *Table 3*. The relative contributions of each parameter to log *P* are given in *Table 4*.

From a comparison of the equations and the relative contributions (shown in *Table 4*) in each solvent/H_2O system, it can be seen that there is no significant difference between the LSER models obtained by the calculated solvatochromic parameters and those obtained by the experimental solvatochromic parameters in all of the three solvent/H_2O systems. The good quality of the solvatochromic parameters calculated by Systahl 2.0 and Pistal 1.0 systems is thus demonstrated.

2.2. *Structural Diversity of the Investigated Solutes.* Experimental limitations restricted the extended set of 154 compounds to 88 solutes whose values of $\log P_{npoe}$, $\log P_{dce}$, and $\log P_{oct}$ together with the structural parameters V_w, π^*, β, and α are shown in *Table 2*. Therefore, it was necessary to compare the parameter distributions of the extended and initial sets, and to check whether the reduced set of 88 compounds still allowed a well-balanced exploration of the 4D-space defined by V_w, π^*, β, and α. *Fig. 2* shows that the extended set (154 compounds) has a broader distribution than the initial set of 80 compounds for all four parameters., The distribution range in the extended set is wider mainly for V_w, π^*, and β. For the final set of 88 compounds, the structural diversity (in terms of V_w, π^*, β, and α) remains as high as for the extended set.

2.3. *Correlations between Partition Coefficients in Different Solvent/Water Systems.* The similarity between the *o*-NPOE/H_2O and DCE/H_2O systems can be seen from the correlation between the partition coefficients in the two solvent systems (*Eqn. 2* and *Fig. 3*):

$$\log P_{npoe} = 0.92(\pm 0.05) \log P_{dce} - 0.26(\pm 0.10) \quad (2)$$

$$n = 88;\ q^2 = 0.94;\ r^2 = 0.94;\ s = 0.30;\ F = 1444$$

The significant correlation between $\log P_{dce}$ and $\log P_{npoe}$ implies that the partitioning of the investigated compounds in the two solvent systems is controlled by similar dominant factors. But the slope and intercept of *Eqn. 2* show that the $\log P_{npoe}$ values are lower than the $\log P_{dce}$ values.

Fig. 4, a, and *Eqn. 3* show the relationship between $\log P_{npoe}$ and $\log P_{oct}$. It can be seen that there is a significantly lower global correlation for the whole set of investigated compounds, indicating different partitioning mechanisms governing the partitioning of solutes in these two solvent systems.

Table 2. *Physicochemical Parameters of the Investigated Compounds*

No.	Solutes[a])	V_w[b])	π^*[c])	β[d])	α[e])	log P_{oct}	log P_{dce}	log P_{npoe}[f])
1	4-$MeC_6H_4CH_2NH_2$	132.0	0.87	0.62	0.16	1.58	1.55	1.80
2	4-$MeC_6H_4CH_2NHMe$	149.5	0.80	0.70	0.08	1.96	2.03	1.48
3	4-$MeC_6H_4CH_2NHCH_2Me$	166.1	0.80	0.70	0.08	2.38	2.48	1.86
4	4-$MeC_6H_4CH_2NH(CH_2)_2Me$	183.4	0.80	0.70	0.08	2.96	3.00	2.36
5	4-$MeC_6H_4CH_2NH(CH_2)_3Me$	199.4	0.80	0.70	0.08	3.49	3.46	2.90
6	4-$MeC_6H_4CH_2NH(CH_2)_4Me$	217.7	0.80	0.70	0.08	4.26	4.17	3.48
7	4-$MeC_6H_4CH_2NH(CH_2)_5Me$	234.2	0.80	0.70	0.08	4.96	5.02	4.07
8	4-$MeC_6H_4CH_2NH(CH_2)_6Me$	251.8	0.80	0.70	0.08	5.12	5.30	4.29
9	4-BrC_6H_4COOH	133.8	0.94	0.40	0.59	2.86	1.04	0.82
10	3-ClC_6H_4COOH	126.2	0.86	0.30	0.59	2.71	0.97	0.94
11	4-ClC_6H_4COOH	126.5	0.86	0.27	0.59	2.06	1.06	0.88
12	4-IC_6H_4COOH	141.6	0.96	0.42	0.59	3.13	1.59	1.46
13	Carprofen	236.4	2.00	0.63	0.87	4.04	2.58	3.01
14	Flurbiprofen	223.1	1.78	0.49	0.60	3.81	2.91	2.94
15	Ibuprofen	197.0	1.14	0.49	0.60	3.87	2.87	2.72
16	Naproxen	216.5	1.64	0.79	0.60	3.06	2.57	2.51
17	Pirprofen	224.6	1.50	0.49	0.60	3.58	2.78	2.61
18	Suprofen	227.6	2.09	1.15	0.60	2.83	2.36	1.76
19	Ketoprofen	239.1	2.12	0.99	0.60	2.77	2.38	1.81
20	Indomethacin	283.5	1.86	1.29	0.60	3.18	2.87	3.03
21	PhCOOH	111.8	0.74	0.40	0.59	1.96	0.72	0.50
22	$PhCH_2COOH$	128.7	1.12	0.45	0.60	1.46	0.60	0.12
23	$Ph(CH_2)_2COOH$	146.0	1.12	0.45	0.60	1.89	1.11	0.51
24	$Ph(CH_2)_3COOH$	162.4	1.12	0.45	0.60	2.42	1.74	1.28
25	$Ph(CH_2)_4COOH$	179.8	1.12	0.45	0.60	2.85	2.27	1.77
26	$Ph(CH_2)_6COOH$	213.6	1.12	0.45	0.60	3.53	3.06	2.52
27	$Ph(CH_2)_7COOH$	230.6	1.12	0.45	0.60	4.09	3.46	2.97
28	Antipyrine	183.5	0.69	1.10	0.00	0.17	0.71	−0.03
29	Diazepam	253.1	2.22	0.86	0.00	2.92	3.67	2.96
30	Homatropine	247.0	1.85	1.76	0.39	1.63	1.61	1.10
31	Nicotine	168.3	1.01	1.25	0.00	1.17	0.74	0.60
32	Phenobarbital	204.5	0.59	1.26	0.20	1.44	0.71	0.02
33	Phenytoin	228.3	1.45	1.02	0.60	2.68	1.62	0.80
34	3-$NO_2C_6H_4OH$	112.9	1.54	0.23	0.79	2.00	0.92	1.10
35	Sulfanilamide	139.1	1.89	1.26	0.60	−0.69	−0.93	−1.02
36	Sulfacetamide	174.8	2.58	1.25	0.33	−0.16	−0.52	−0.64
37	Sulbenzamide	233.6	2.48	1.25	0.33	1.46	1.52	1.05
38	Sulfapyridine	209.4	2.76	1.78	0.33	0.02	0.30	−0.21
39	Sulfamethazine	237.5	2.72	1.90	0.33	0.25	0.80	0.12
40	Sulfisomidine	239.0	2.72	1.90	0.33	−0.37	−0.73	−1.22
41	Sulfamethoxypyridazine	229.6	2.93	2.38	0.33	0.35	0.73	−0.08
42	Sulfacytine	243.9	1.99	2.16	0.36	−0.20	0.35	−0.45
43	Sulfadoxine	254.6	3.14	2.35	0.06	0.56	1.67	0.69
44	Sulfadimethoxine	254.4	3.14	2.50	0.33	1.40	1.79	1.34
45	Sulfathiazole	199.1	2.69	1.86	0.46	0.00	−0.37	−0.38
46	Sulfamethoxazole	207.5	2.59	1.64	0.36	0.72	0.98	0.52
47	Sulfamoxole	222.7	2.59	1.68	0.36	−0.14	−0.29	0.12
48	Sulfamethizole	211.7	2.25	1.46	0.36	0.55	0.22	−0.48
49	Sulfaphenazole	272.6	3.48	1.69	0.36	1.27	1.53	0.98
50	$MeCO_2Me$	71.2	0.55	0.45	0.00	0.18	0.79	0.28
51	$MeCO_2Et$	88.5	0.55	0.45	0.00	0.73	1.34	0.91
52	$MeCO_2Bu$	123	0.55	0.45	0.00	1.82	2.48	1.86

Table 2 (cont.)

53	MeCN	47.3	0.65	0.36	0.00	− 0.34	0.30	− 0.22
54	$MeCH_2CN$	64.6	0.65	0.36	0.00	0.10	0.94	0.27
55	$MeCON(Me_2)$	94.0	1.30	0.78	0.00	− 0.77	− 0.43	− 0.64
56	EtOH	52.5	0.40	0.48	0.37	− 0.25	− 1.00	− 1.29
57	PrOH	70.1	0.40	0.48	0.37	0.28	− 0.38	− 0.76
58	$C_5H_{11}OH$	104.5	0.40	0.48	0.37	1.40	0.72	0.39
59	$C_6H_{13}OH$	121.6	0.40	0.48	0.37	2.03	1.22	0.94
60	BuCOOH	105.3	0.55	0.45	0.60	1.39	0.23	− 0.06
61	$BuNO_2$	99.1	0.79	0.32	0.00	1.47	2.61	1.99
62	$PhCOCH_3$	122.3	1.12	0.51	0.00	1.58	2.38	2.00
63	$PhNO_2$	107.6	1.01	0.28	0.00	1.85	3.13	2.44
64	$2\text{-}ClC_6H_4NO_2$	122.0	1.13	0.28	0.00	2.24	3.32	2.88
65	$PhCH_2CN$	121.5	1.22	0.45	0.00	1.56	3.40	2.12
66	$PhCH_2COMe$	139.0	1.26	0.51	0.00	1.44	2.49	1.86
67	$PhCH_2CH_2OCOMe$	163.7	1.12	0.45	0.00	2.30	3.25	2.54
68	Pyridine	82.5	0.87	0.52	0.00	0.65	0.72	0.26
69	Acridine	174.9	1.57	0.52	0.00	3.40	3.57	3.61
70	Naphthalene-1-carboxylic acid	158.5	1.05	0.40	0.59	3.10	2.05	1.81
71	Naphthalen-1-amine	144.1	1.25	0.57	0.06	2.28	3.08	2.49
72	$PhNH_2$	98.0	0.94	0.41	0.06	0.90	1.45	1.08
73	$PhNHC_2H_5$	133.0	0.78	0.45	0.03	2.16	3.00	2.36
74	$2\text{-}ClC_6H_4NH_2$	111.8	1.06	0.41	0.06	1.91	2.54	2.12
75	$2\text{-}NH_2C_6H_4Ph$	173.9	1.55	0.41	0.18	2.84	3.45	3.20
76	[1,1′-Biphenyl]-4,4′-diamine	185.0	1.90	0.82	0.12	1.53	2.23	1.82
77	$4\text{-}NO_2C_6H_4NH_2$	118.3	1.89	0.38	0.42	1.39	1.70	1.52
78	PhOH	93.8	0.72	0.30	0.60	1.49	0.61	0.58
79	$3\text{-}ClC_6H_4OH$	107.8	0.84	0.16	0.69	2.49	1.28	1.48
80	$3\text{-}CH_3C_6H_4COOH$	128.8	0.72	0.40	0.59	2.37	1.33	1.01
81	$3\text{-}ClC_6H_4CH_2COOH$	143.3	1.24	0.45	0.60	2.09	1.24	0.93
82	$PhCH_2OH$	111.6	0.84	0.58	0.33	1.08	0.79	0.36
83	$4\text{-}ClC_6H_4CH_2OH$	126.3	0.96	0.58	0.33	1.96	1.50	1.27
84	$4\text{-}NO_2C_6H_4OH$	113.9	1.74	0.26	0.82	1.92	0.79	0.94
85	MeSOMe	71.0	1.00	0.76	0.00	− 1.35	− 1.57	− 1.42
86	Et_3N	126.1	0.14	0.73	0.00	1.36	1.21	0.81
87	$PhCH_2NMe_2$	150.9	0.71	0.73	0.00	1.91	2.46	1.64
88	$C_9H_{19}COOH$	188.7	0.55	0.45	0.60	4.09	3.16	2.94

[a]) The structures of complex compounds are shown in *Fig. 1*. [b]) *Van der Waals* volume of the compounds (calculated by MOLSV) and atomic radii of *Gavezzotti* [30]. [c]) Dipolarity/polarizability of the compounds, calculated by the Pistal 1.0 fragmental system [32]. [d]), [e]) H-Bond-acceptor basicity and H-Bond-donor acidity, calculated by the Systahl 2.0 fragmental system [31]. [f]) Compounds **1**–**27**, **29**–**31**, **33**, **34**, **37**, **43**, **49**, **60**, **69**–**71**, **75**, and **86**–**88** measured by the potentiometric method, $n = 2$ or 3, $SD \leq 0.05$; the others by the shake-flask method, $n = 3$, $SD \leq 0.08$, except for compounds **28**, **35**, **45**, **48**, **55**, **56**, and **85**, $n = 3$, $0.13 \leq SD \leq 0.30$.

$$\log P_{npoe} = 0.83(\pm 0.10) \log P_{oct} - 0.23(\pm 0.21) \quad (3)$$
$$n = 88; q^2 = 0.77; r^2 = 0.78; s = 0.61; F = 303$$

2.4. *LSERs Model of* o-*NPOE/H_2O Partition Coefficients of the Reduced Set of 88 Compounds.* LSERs were applied to the partition coefficients of the set of 88 compounds in *o*-NPOE/H_2O (*Table 2*), yielding *Eqn. 4:*

Table 3. *Regression Coefficients* (± 95% confidence limits) *of LSERs Equations of 41 Compounds and Regression Statistics.*

	$\log P = v \cdot V_w + p \cdot \pi^* + a \cdot \alpha + b \cdot \beta + c$									
$\log P$[a])	v	p	b	a	c	n[b])	q^2[c])	r^2[d])	s[e])	F[f])
$T \log P_{npoe}$	$3.19 \cdot 10^{-2}$	0.04	− 4.97	− 2.39	0.27	41	0.93	0.94	0.30	147
	$\pm 0.37 \cdot 10^{-2}$	± 0.23	± 0.59	± 0.45	± 0.35					
$\log P_{npoe}$	$3.14 \cdot 10^{-2}$	0.08	− 4.31	− 2.24	− 0.03	41	0.91	0.93	0.32	127
	$\pm 0.35 \cdot 10^{-2}$	± 0.31	± 0.70	± 0.40	± 0.63					
$T \log P_{dce}$	$3.41 \cdot 10^{-2}$	− 0.13	− 5.32	− 3.04	0.87	41	0.92	0.94	0.34	136
	$\pm 0.44 \cdot 10^{-2}$	± 0.26	± 1.04	± 0.41	± 0.35					
$\log P_{dce}$	$3.34 \cdot 10^{-2}$	− 0.12	− 4.70	− 2.89	0.66	41	0.92	0.94	0.33	141
	$\pm 0.30 \cdot 10^{-2}$	± 0.27	± 0.76	± 0.42	± 0.57					
$T \log P_{oct}$	$3.18 \cdot 10^{-2}$	− 0.58	− 3.61	0.07	− 0.01	41	0.92	0.94	0.29	136
	$\pm 0.34 \cdot 10^{-2}$	± 0.20	± 0.68	± 0.39	± 0.42					
$\log P_{oct}$	$3.02 \cdot 10^{-2}$	− 0.53	− 3.02	0.23	− 0.15	41	0.90	0.92	0.32	109
	$\pm 0.37 \cdot 10^{-2}$	± 0.30	± 0.74	± 0.39	± 0.64					

[a]) $T \log P$: $\log P$ calculated by calculated solvatochromic parameters. [b]) The number of compounds. [c]) Cross-validated correlation coefficient [37]. [d]) Squared correlation coefficient. [e]) Standard deviation. [f]) *Fisher*'s test.

Table 4. *The Relative Contributions of Each Structural Parameter to the LSERs Equations of 41 Compounds*

$\log P$[a])	% V_w	% π^*	% β	% α
$T \log P_{npoe}$	45.0	0.6	28.4	25.9
$\log P_{npoe}$	44.3	2.7	29.2	23.9
$T \log P_{dce}$	42.3	1.9	26.8	28.9
$\log P_{dce}$	43.1	1.7	27.3	27.9
$T \log P_{oct}$	58.7	11.4	26.5	3.4
$\log P_{oct}$	58.9	12.9	27.2	1.0

[a]) $T \log P$: $\log P$ obtained from calculated solvatochromic parameters.

$$\log P_{npoe} = 2.43 \cdot 10^{-2}(\pm 0.32 \cdot 10^{-2}) \cdot V_w + 0.19(\pm 0.36) \cdot \pi^* - 2.72(\pm 0.60) \cdot \beta - 1.85(\pm 0.51) \cdot \alpha - 0.23(\pm 0.37) \quad (4)$$

$$n = 88; q^2 = 0.75; r^2 = 0.79; s = 0.60; F = 78$$

Compounds antipyrine (**28**), sulfisomidine (**40**), and sulfadimethoxine (**44**) were poorly predicted by *Eqn. 4*, as illustrated by the higher statistical quality of *Eqn. 5, a* when these solutes are omitted:

$$\log P_{npoe} = 2.50 \cdot 10^{-2}(\pm 0.30 \cdot 10^{-2}) \cdot V_w + 0.13(\pm 0.34) \cdot \pi^* - 2.78(\pm 0.50) \cdot \beta - 1.94(\pm 0.49) \cdot \alpha - 0.19(\pm 0.34) \quad (5a)$$

$$n = 85; q^2 = 0.82; r^2 = 0.85; s = 0.50; F = 112$$

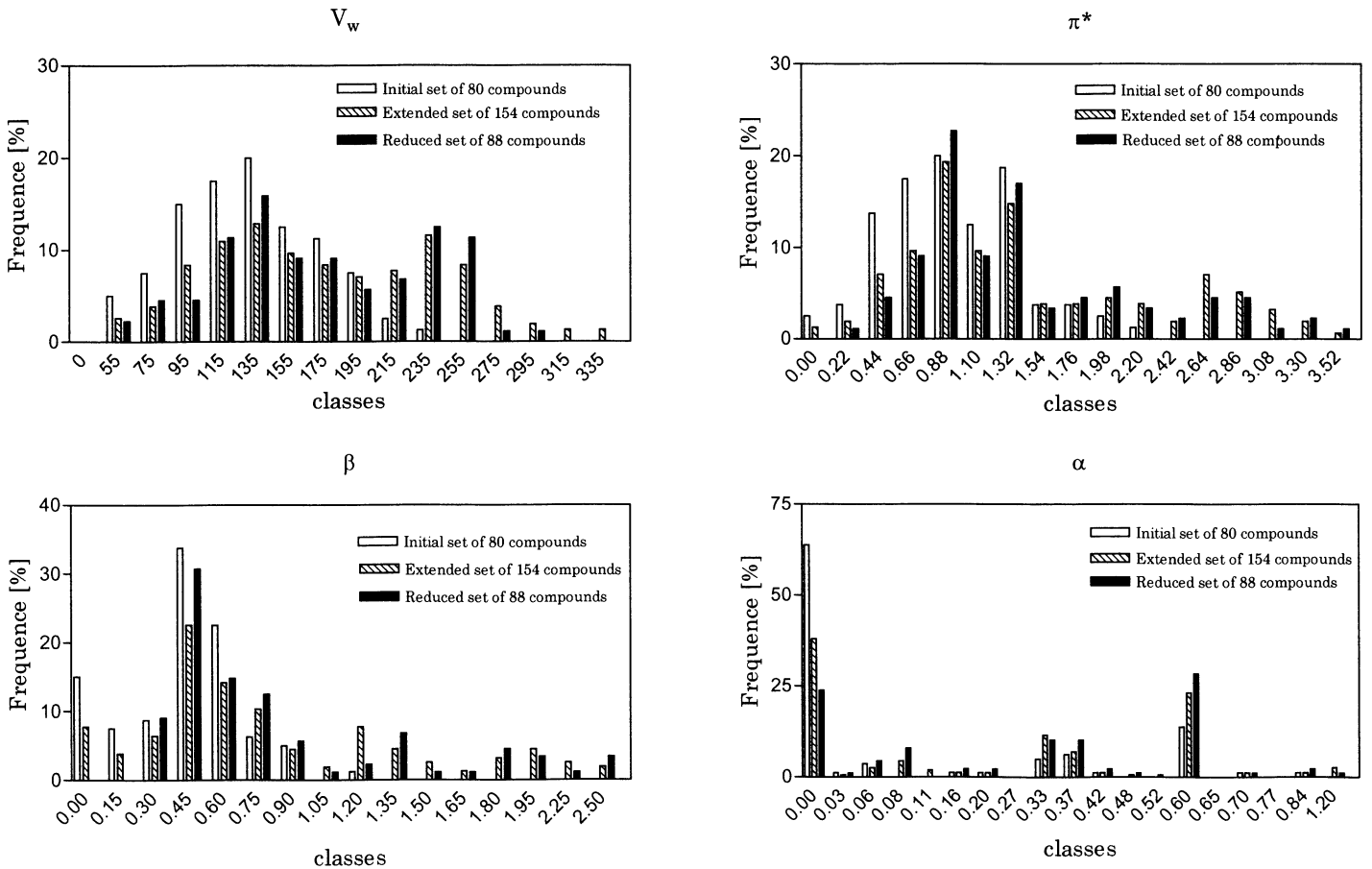

Fig. 2. *Distribution of compounds in the parameter space for the initial set of 80 compounds, the extended set of 154 compounds, and the reduced set of 88 compounds*

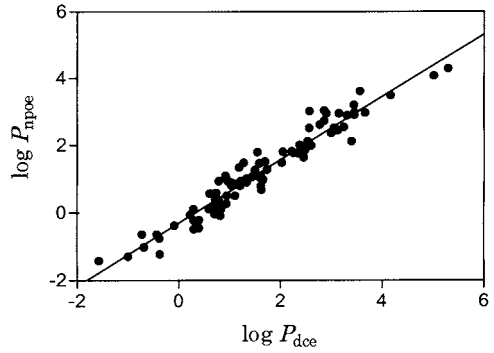

Fig. 3. *Relationship between log* P_{npoe} *and log* P_{dce} *values of the compounds investigated*

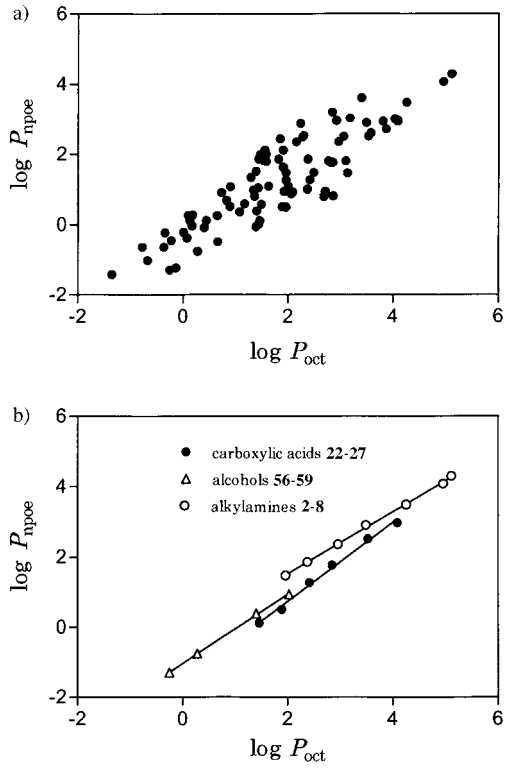

Fig. 4. *The relationship between log* P_{oct} *and log* P_{npoe}*:* a) *for the whole set of compounds investigated:* b) *for three special sets of compounds*

The poor prediction of log P_{npoe} of sulfadimethoxine (**44**) can be attributed to a non-negligible error in experimental measurements. Indeed, this compound has very low solubility in H_2O, making it impossible to measure its log P_{npoe} by potentiometry. In the shake-flask experiments, the very low initial concentration of buffer solution (lower

than 10^{-4} M) caused large errors in concentration determination by UV detection, producing large errors in log P_{npoe} value. The reason for the poor prediction of log P_{npoe} of the other two outliers, **28** and **40**, is unclear and is under investigation.

The standardization of *Eqn. 5, a* gives the relative contributions of each variable to the LSER model, namely 41.5% for V_w, 2.7% for π^*, 41.1% for β, and 14.6% for α, indicating that the governing factors in *o*-NPOE/H_2O partitioning are V_w and β, while α is of lower importance. The π^* contribution has no statistical significance in this solvent system. *Eqn. 5, b* shows the LSER model when π^* is removed in the solvatochromic analysis.

$$\log P_{npoe} = 2.54 \cdot 10^{-2}\left(\pm 0.28 \cdot 10^{-2}\right) \cdot V_w - 2.66(\pm 0.43) \cdot \beta - 1.88(\pm 0.43) \cdot \alpha - 0.18(\pm 0.33) \quad (5b)$$

$$n = 85; q^2 = 0.83; r^2 = 0.85; s = 0.50; F = 149$$

The LSER model for the partition coefficients of the reduced set of 88 compounds in *o*-NPOE/H_2O gives important information on the intermolecular forces controlling the partitioning of neutral organic solutes in this system. Partitioning is the balance of interactions between the *o*-NPOE and H_2O phases. The negative regression coefficients of α and β imply that *o*-NPOE is less capable of donating and accepting H-bonds than is H_2O. Intermolecular interactions encoded by β can be expressed only in H_2O (considering concentration of H_2O in *o*-NPOE at saturation; see *Table 1*). The non-significance of the π^* parameter suggests that intermolecular interactions encoded by this parameter operate with equal strength in the *o*-NPOE and H_2O phases.

To compare the partitioning mechanisms in different solvent/H_2O systems, LSERs were also applied to log P_{dce} and log P_{oct} for the same set of compounds (*Table 2*). *Eqns. 6, a* and *7, a* were obtained:

$$\log P_{dce} = 2.71 \cdot 10^{-2}(\pm 0.34 \cdot 10^{-2}) \cdot V_w + 0.01(\pm 0.35) \cdot \pi^* - 2.67(\pm 0.56) \cdot \beta - 2.54(\pm 0.49) \cdot \alpha + 0.15(\pm 0.39) \quad (6a)$$

$$n = 85; q^2 = 0.82; r^2 = 0.85; s = 0.54; F = 111$$

$$\log P_{oct} = 2.74 \cdot 10^{-2}(\pm 0.29 \cdot 10^{-2}) \cdot V_w - 0.54(\pm 0.24) \cdot \pi^* - 2.37(\pm 0.48) \cdot \beta + 0.15(\pm 0.41) \cdot \alpha - 0.12(\pm 0.27) \quad (7a)$$

$$n = 85; q^2 = 0.88; r^2 = 0.90; s = 0.44; F = 177$$

After removal of the term with no significance:

$$\log P_{dce} = 2.70 \cdot 10^{-2}(\pm 0.32 \cdot 10^{-2}) \cdot V_w - 2.68(\pm 0.49) \cdot \beta - 2.55(\pm 0.42) \cdot \alpha + 0.15(\pm 0.39) \quad (6b)$$

$$n = 85; q^2 = 0.82; r^2 = 0.85; s = 0.54; F = 150$$

$$\log P_{oct} = 2.76 \cdot 10^{-2}(\pm 0.27 \cdot 10^{-2}) \cdot V_w - 0.51(\pm 0.22) \cdot \pi^* - 2.36(\pm 0.44) \cdot \beta - 0.11(\pm 0.27) \quad (7b)$$

$$n = 85; q^2 = 0.88; r^2 = 0.90; s = 0.44; F = 237$$

Eqn. 6, a and the relative contributions of each variable to $\log P_{dce}$, namely 43.3% for V_w, 0.1% for π^*, 38.1% for β, and 18.6% for α, indicate the close analogy between $\log P_{npoe}$ and $\log P_{dce}$. It is thus concluded that partitioning of the investigated compounds in *o*-NPOE/H_2O and DCE/H_2O is controlled by the same structural properties. This further confirms the result (*Eqn. 2*) in *Sect. 2.3*. But it should be noted that the regression coefficient of α in *o*-NPOE/H_2O (*Eqn. 5, a*) is slightly lower than that in DCE/H_2O (*Eqn. 6, a*) due to the higher ability of *o*-NPOE to accept H-bond compared to DCE.

In *Eqn. 7, a*, the relative contributions of each variable to $\log P_{oct}$ are 49.0% for V_w, 12.1% for π^*, 37.7% for β, and 1.2% for α, implying that V_w and β are the most important structural descriptors contributing to $\log P_{oct}$, while π^* is of secondary importance, and α has no statistical significance in octanol/H_2O. From a comparison with the relative contributions of structural descriptors in the two other solvent systems, it can be seen that a different partitioning mechanism exists in octanol/H_2O.

The difference between intermolecular interactions encoded in octanol/H_2O and *o*-NPOE/H_2O ($\Delta\log P$) can be quantified by *Eqn. 8* with relative contributions of 9.7% for V_w, 35.1% for π^*, 15.5% for β, and 39.7% for α, indicating that π^* and α are the main structural properties responsible for the difference.

$$\Delta \log P_{oct-npoe} = 0.23 \cdot 10^{-2}(\pm 0.20 \cdot 10^{-2}) \cdot V_w - 0.67(\pm 0.19) \cdot \pi^* + 0.42(\pm 0.30) \cdot \beta + 2.08(\pm 0.30) \cdot \alpha + 0.06(\pm 0.23)) \quad (8)$$

$$n = 85; q^2 = 0.71; r^2 = 0.75; s = 0.33; F = 59$$

The same equation for $\Delta\log P_{oct-dce}$ is given by *Eqn. 9, a* with relative contributions of 1.2% for V_w, 30.6% for π^*, 12.3% for β, and 55.9% for α:

$$\Delta \log P_{oct-dce} = 0.03 \cdot 10^{-2}(\pm 0.18 \cdot 10^{-2}) \cdot V_w - 0.54(\pm 0.22) \cdot \pi^* + 0.30(\pm 0.38) \cdot \beta + 2.69(\pm 0.37) \cdot \alpha - 0.28(\pm 0.25) \quad (9a)$$

$$n = 85; q^2 = 0.76; r^2 = 0.79; s = 0.37; F = 74$$

When nonsignificant structural parameters were removed:

$$\Delta \log P_{oct-dce} = 0.35(\pm 0.09) \cdot \pi^* + 2.59(\pm 0.34) \cdot \alpha - 0.22(\pm 0.19) \quad (9b)$$

$$n = 85; q^2 = 0.76; r^2 = 0.77; s = 0.38; F = 138$$

In other words, $\Delta\log P_{\text{oct-npoe}}$ and $\Delta\log P_{\text{oct-dce}}$ encode comparable structural information as confirmed by *Eqn. 10:*

$$\Delta\log P_{\text{oct-npoe}} = 0.76(\pm0.07)\Delta\log P_{\text{oct-dce}} + 0.43(\pm0.06) \quad (10)$$

$$n = 88; q^2 = 0.82; r^2 = 0.83; s = 0.26; F = 420$$

The lower correlation coefficient between $\log P_{\text{npoe}}$ and $\log P_{\text{oct}}$ (*Eqn. 3*, $r^2 = 0.78$) is understandable since different mechanisms govern the partitioning of solutes in these two solvent systems. From the result of the solvatochromic analysis, it is known that the difference between the two partition coefficients mainly comes from the relative contributions of two structural descriptors π^* and α. This point is confirmed by the much higher quality of the correlation when these two descriptors are included in *Eqn. 10:*

$$\log P_{\text{npoe}} = 0.96(\pm0.07)\log P_{\text{oct}} - 1.90(\pm0.36)\cdot\pi^* + 0.28(\pm0.12)\cdot\alpha - 0.24(\pm0.20) \quad (11)$$

$$n = 85; q^2 = 0.90; r^2 = 0.91; s = 0.39; F = 291$$

Eqn. 11 implies that compounds possessing the same values for π^* and α should have similar partitioning behavior in the two solvent systems, as indeed is seen in the good correlations between $\log P_{\text{oct}}$ and $\log P_{\text{npoe}}$ for three separate sets of compounds in *Fig. 4, b*. The three sets are alkylamines **2**–**8**, carboxylic acids **22**–**27**, and alcohols **56**–**59**. The compounds in each of the three sets have the same values of π^* and α.

The correlations between $\log P_{\text{oct}}$ and $\log P_{\text{npoe}}$ for the three sets of compounds were given by *Eqn. 12* for alkylamines **2**–**8**, *Eqn. 13* for carboxylic acids **22**–**27**, and *Eqn. 14* for alcohols **56**–**59**.

$$\log P_{\text{npoe}} = 0.87(\pm0.04)\log P_{\text{oct}} - 0.22(\pm0.13) \quad (12)$$

$$n = 7; q^2 = 0.998; r^2 = 0.999; s = 0.05; F = 3966$$

$$\log P_{\text{npoe}} = 1.12(\pm0.12)\log P_{\text{oct}} - 1.50(\pm0.35) \quad (13)$$

$$n = 6; q^2 = 0.983; r^2 = 0.994; s = 0.10; F = 629$$

$$\log P_{\text{npoe}} = 0.99(\pm0.09)\log P_{\text{oct}} - 1.03(\pm0.11) \quad (14)$$

$$n = 4; q^2 = 0.996; r^2 = 0.999; s = 0.04; F = 2289$$

The slopes and intercepts are different in these three equations mainly because the values of π^* and α are different in the three sets.

3. Conclusions. – Partition coefficients in *o*-NPOE/H_2O were analyzed for the intermolecular forces they encode. The LSER models obtained identify *Van der Waals* volume (V_w), H-bond-accepting capacity (β), and H-bond-donating capacity (α) as the three molecular descriptors of solutes determining their $\log P_{\text{npoe}}$ values. The partitioning mechanism of the investigated compounds in *o*-NPOE/H_2O is controlled by the same structural properties as in DCE/H_2O, but is different than in octanol/H_2O mainly due to the different relative contributions of π^* and α in the two solvent systems.

The parameters $\Delta\log P_{\text{oct-npoe}}$ and $\Delta\log P_{\text{oct-dce}}$ express mainly the H-bond donor acidity (α) and dipolarity/polarizability (π^*) of a solute.

The solvent *o*-NPOE is a good candidate to replace DCE in lipophilicity measurements, since it has better physicochemical properties such as lower volatility, lower solubility in H_2O, lower vapor pressure, and no known toxicity.

Experimental Part

1. *Solutes.* The (4-methylbenzyl)alkylamines were synthesized by known procedures [29] and kindly offered by the research group of Prof. *R. Fruttero* (Department of Pharmaceutical Sciences and Technology, University of Turin, Italy). All other compounds were obtained from commercial sources (*Merck*, Darmstadt, Germany; *Fluka*, Buchs, Switzerland; *Janssen*, Beerse, Belgium; *Aldrich*, Steinheim, Germany; *Sigma Chemie*, Buchs, Switzerland; *Lancaster Synthesis*, Morecombe, England; *ICN*, Aurora, USA) and in the highest available purity. Anal.-grade *o*-nitrophenyl octyl ether was purchased from *Fluka*. Distilled H_2O was used throughout.

No evidence was found from the literature about the toxicity of *o*-NPOE. However, all precautions were taken to avoid skin contact by using rubber gloves, since skin permeation is possible and might lead to toxic metabolites.

2. *Computational Details.* The LSERs models were generated by multivariate regression with both the TSAR program (*Oxford Molecular*, Oxford, GB) and the QSAR module in the Sybyl software (*Tripos Associates*, St-Louis, MO, USA), running on *Silicon Graphics Indy R4400* 175 MHz, *O_2 R5000* 180 MHz, and *Origin 2000 R10000* 195 MHz workstations. *Van der Waals* volumes (V_w) were calculated with the standard software MOLSV (QCPE No. 509) and the atomic radii of *Gavezzotti* [30]. The solvatochromic parameters were calculated by Systahl 2.0 (for β and α) and Pistal 1.0 (for π^*) fragmental systems. The Systahl 2.0 fragmental system [31] identifies the structural elements (polar H-atoms and lone pairs) able to form H-bonds, and assigns a fragmental value to each of them. The total capacity of a solute to donate (α) or accept H-bonds (β) is given by the sum of the donor or acceptor capacity of its constitutive H-bonding elements (polar H-atoms or lone pairs). The Pistal 1.0 fragmental system [32] is associated with a research algorithm to compute automatically the π^* values for any compound, in which the global value of a molecule is obtained by summing the partial contributions of its fragments.

The relative contributions of each variable to the LSERs models were obtained by a standardization procedure [33].

3. *Selection of the Compounds Used for Solvatochromic Analysis.* The set used in this study was an expansion of the original set of 80 compounds [28] obtained by adding 74 more compounds to cover a broader range in the distribution of the structural parameters V_w, π^*, β, and α (*Fig. 2*). The 154 compounds were rigid ones and included drug molecules. However, the set had to be reduced to 88 compounds (*Table 2*) in this study due to the lack of availability of some compounds, the experimentally inaccessible high or low $\log P_{\text{npoe}}$ values of others, and other experimental limitations.

4. *Measurements of log* P_{npoe} *Values.* 4.1. *Shake-Flask Experiments.* The partition coefficients in *o*-NPOE/H_2O were measured by the shake-flask method for all nonionizable compounds, and for some hydrophilic or poorly H_2O-soluble ionizable compounds. A 0.02M phosphate buffer containing 0.15M KCl was used. The phosphate buffer was adjusted to pH 7 for the nonionizable compounds and to a pH value where the neutral form was in large excess for the ionizable compounds. Both *o*-NPOE and phosphate buffer were mutually saturated by stirring the two phases vigourously for 6 h. After phase separation in a separation funnel, the two phases were collected and centrifuged at 2500 rpm for 20 min (*MSE Mistral 2000* centrifuge, UK) to remove the last drops of the other phase.

Drug solutions (0.1 to 1 mM) in *o*-NPOE-saturated phosphate buffer were prepared. Three volume ratios of drug soln. to buffer-saturated *o*-NPOE were used. After gentle shaking overnight, the two phases were separated by centrifugation at 4000 rpm for 20 min. Sample concentrations were determined in both phases for most compounds or only in the aq. phase for some hydrophilic compounds, since the *o*-NPOE phase must be diluted at least 20 times by the mobile phase before HPLC injection, and this made the concentration of some hydrophilic compounds in *o*-NPOE too low to be detected.

The experimental precision of log P_{npoe} values was good for the compounds with positive log P_{npoe} values (SD ≤ 0.08), but, for some hydrophilic compounds with negative log P_{npoe} values, the experimental precision became lower (SD is as large as 0.30 for compounds **55** and **85**).

For UV-active compounds, the concentration measurements were performed by HPLC with a liquid chromatograph *Waters 2690* Separation module (*Waters*, Milford, MA, USA) equipped with a *Waters 2487* dual wavelengths absorbance detector set at the λ_{max} of each compound. The column used was a *Symmetry® C8* 3.5 μm (3.0 × 150 mm, *Waters*, Milford, MA, USA). The mobile phase was the mixture of 0.02M phosphate buffer (adjusted to a pH value where the compound was neutral) and MeCN. The phosphate buffer was filtered through 0.45-μm *HA Millipore* filters (*Millipore*, Milford, MA, USA).

For UV-inactive compounds, a gas chromatograph–mass spectrometer (GC/MS) (*Hewlett-Packard*, Palo Alto, CA, USA) was used for the concentration measurements with He as carrier gas in a *CAM* column (30 m × 0.25 mm, 0.5 μm, *J&W*, Folsom, CA, USA).

The shake-flask method is a conventional procedure for log *P* measurements. However, it is limited to the range $-3 < \log P < 3$. Beyond these limits, log *P* values assessed by this method become unreliable [34].

4.2. *Potentiometric Experiments.* The partition coefficients of some ionizable compounds in *o*-NPOE/H_2O were determined with a *GLpKa* apparatus (*Sirius Analytical Instruments*, Forest Row, East Sussex, UK). All titrations were conducted at $25 \pm 0.5°$ and under a slow Ar flow to avoid CO_2 absorption. The *o*-NPOE phase was presaturated with 0.15M KCl and added manually to the titration vial. Two or three titrations were made with different *o*-NPOE/H_2O ratios. The volume ratio of *o*-NPOE phase to aq. phase was between 0.005 and 0.5. A higher ratio was not possible because the mixture emulsified under stirring and the electrode did not work well under those conditions. This makes the measurement of partition coefficients impossible by this method for hydrophilic compounds whose log *P* values are negative. Thus, the shake-flask method was used for these ionizable compounds.

It should be noted that a much smaller volume of *o*-NPOE can be used (0.1 ml) than that of DCE (at least 1 ml) due to the lower volatility of *o*-NPOE compared to DCE. The potentiometric method gave a good experimental precision in log P_{npoe} values (SD ≤ 0.05) for all compounds tested by this method. The principles and detailed experimental procedures of the potentiometric method can be found elsewhere [35][36].

P. A. C., G. B., and *H. H. G.* are indebted to the *Swiss National Science Foundation* for support. The authors thank also Dr. *Sébastien Rey* for his help in the parameterization of Systahl 2.0.

REFERENCES

[1] H. van de Waterbeemd, B. Testa, in 'Advances in Drug Research', Ed. B. Testa, Academic Press, London, 1987, Vol. 16, p. 87–227.
[2] H. van de Waterbeemd, in 'Hydrophobicity of Organic Compounds', Ed. F. Darvas, CompuDrug International, Vienna, 1986.
[3] C. Hansch, A. Leo, 'Substituent Constants for Correlation Analysis in Chemistry and Biology', John Wiley and Sons, New York, 1979.
[4] I. Komiya, J. Y. Park, A. Kamani, N. F. H. Ho, W. I. Higuchi, *Int. J. Pharm.* **1980**, *4,* 249.
[5] D. C. Taylor, R. Pownall, W. Burke, *J. Pharm. Pharmacol.* **1985**, *37,* 280.
[6] V. A. Levin, *J. Med. Chem.* **1980**, *23,* 682.
[7] P. Artursson, *J. Pharm. Sci.* **1990**, *79,* 476.
[8] A. Buur, L. Trier, C. Magnusson, P. Artursson, *Int. J. Pharm.* **1996**, *129,* 223.
[9] A. R. Hilgers, R. A. Conradi, P. S. Burton, *Pharm. Res.* **1990**, *7,* 902.
[10] L. Hovgaard, H. Brondsted, A. Buur, H. Bundgaard, *Pharm. Res.* **1995**, *12,* 387.
[11] M. S. Roberts, W. J. Pugh, J. Hadgraft, A. C. Watkinson, *Int. J. Pharm.* **1995**, *126,* 219.
[12] M. S. Roberts, W. J. Pugh, J. Hadgraft, *Int. J. Pharm.* **1996**, *132,* 23.
[13] W. J. Pugh, M. S. Roberts, J. Hadgraft, *Int. J. Pharm.* **1996**, *138,* 149.

[14] O. A. Raevsky, V. I. Fetisov, E. P. Trepalina, J. W. McFarland, K. J. Schaper, *Quant. Struct.-Act. Relat.* **2000**, *19,* 366.
[15] F. Wohnsland, B. Faller, *J. Med. Chem.* **2001**, *44,* 923.
[16] S. Okada, H. Nakahara, C. Yomota, K. Mochida, *Chem. Pharm. Bull.* **1985**, *33,* 4916.
[17] D. E. Leahy, J. J. Morris, P. J. Taylor, A. R. Wait, *J. Chem. Soc., Perkin Trans. 2* **1992**, 723.
[18] D. E. Leahy, J. J. Morris, P. J. Taylor, A. R. Wait, *J. Chem. Soc., Perkin Trans. 2* **1992**, 705.
[19] M. J. Kamlet, R. M. Doherty, M. H. Abraham, Y. Marcus, R. W. Taft, *J. Phys. Chem.* **1988**, *92,* 5244.
[20] M. H. Abraham, H. S. Chadha, in 'Lipophilicity in Drug Action and Toxicology', Eds. V. Pliska, B. Testa, and H. van de Waterbeemd, VCH Publishers, Weinheim, 1996, p. 311 – 337.
[21] M. H. Abraham, *Chem. Soc. Rev.* **1993**, 73.
[22] N. El Tayar, R. S. Tsai, B. Testa, P. A. Carrupt, A. Leo, *J. Pharm. Sci.* **1991**, *80,* 590.
[23] A. Pagliara, G. Caron, G. Lisa, W. Fan, P. Gaillard, P. A. Carrupt, B. Testa, M. H. Abraham, *J. Chem. Soc., Perkin Trans. 2* **1997**, 2639.
[24] G. Steyaert, G. Lisa, P. Gaillard, G. Boss, F. Reymond, H. H. Girault, P. A. Carrupt, B. Testa, *J. Chem. Soc., Faraday Trans.* **1997**, *93*, 401.
[25] Z. Samec, J. Langmaier, A. Trojanek, *J. Electroanal. Chem.* **1996**, *409*, 1.
[26] Z. Samec, J. Langmaier, A. Trojanek, E. Samcova, J. Malek, *Anal. Sci.* **1998**, *14*, 35.
[27] O. Valent, J. Koryta, M. Panoch, *J. Electroanal. Chem. Interfacial Electrochem.* **1987**, *226*, 21.
[28] A. Pagliara, E. Khamis, A. Trinh, P. A. Carrupt, R. S. Tsai, B. Testa, *J. Liquid Chromatogr.* **1995**, *18*, 1721.
[29] W. R. Meindl, E. von Angerer, H. Schönenberger, G. Ruckdeschel, *J. Med. Chem.* **1984**, *27*, 1111.
[30] A. Gavezzotti, *J. Am. Chem. Soc.* **1983**, *105*, 5220.
[31] S. Rey, G. Caron, G. Ermondi, P. Gaillard, A. Pagliara, P. A. Carrupt, B. Testa, *J. Mol. Graphics Model.* **2001**, *19*, 521.
[32] S. Rey, ' Hydrogen-bonds and Other Recognition Forces in Molecular Modeling', Ph.D. Thesis, University of Lausanne, 2002.
[33] H. Mager, A. Barth, *Pharmazie* **1979**, *34*, 557.
[34] H. van de Waterbeemd, M. Kansy, B. Wagner, H. Fischer, in 'Lipophilicity in Drug Action and Toxicology', Eds. V. Pliska, B. Testa, and H. van de Waterbeemd, VCH Publishers, Weinheim, 1996, p. 73 – 87.
[35] A. Avdeef, *Quant. Struct.-Act. Relat.* **1992**, *11*, 510.
[36] A. Avdeef, *J. Pharm. Sci.* **1993**, *82,* 183.
[37] M. Baroni, G. Costantino, G. Cruciani, D. Riganelli, R. Valigi, S. Clementi, *Quant. Struct.-Act. Relat.* **1993**, *12,* 9.

Received July 23, 2003